New Model of Wood Cell Wall Microfibril and Its Implications

Umesh P. Agarwal, [1] Sally A. Ralph,[1] Rick S. Reiner,[1] Carlos Baez,[1]

[1] USDA, Forest Service, Forest Products Laboratory, Madison, WI USA

ABSTRACT

Traditionally it has been accepted that the cell walls are made up of microfibrils which are partly crystalline. However, based on the recently obtained Raman evidence that showed that the interior of the microfibril was significantly disordered and water accessible, a new model is proposed. In this model, the molecular chains of cellulose are still organized along the fibril direction but, at the local level, the chains retain significant degrees of freedom. The new fibril model has implications for not only formation of inter-chain H-bonds and therefore, cellulose ultrastructure but also, a number of areas of practical applications where cellulose fibers are used. Various research and development areas, including biofuels and nanocellulose fields, are likely to be impacted. Based on the new model, the broadened nature of X-ray diffractograms of cellulose I materials and lack of crystallinity increase upon pulp and cellulose nanocrystals (CNCs) production were interpreted in terms of degree of consolidation of cellulose chains within the microfibrils rather than their crystallite size.

KEYWORDS

Cell wall, Cellulose, Crystallinity, Microfibril, Raman spectroscopy, X-ray diffraction

INTRODUCTION

Plant cellulose, which is synthesized in the context of biological function and in the presence of other cell wall constituents, is one of the most abundant materials in nature. The knowledge of cellulose structure is central to not only understanding molecular architecture and mechanics of cell walls but also for making advances in a number of multidisciplinary fields. For example, in the area of biofuels where the cell wall needs to be deconstructed enzymatically and cellulose needs to be converted to glucose before being fermented to ethanol, it is known that cellulose ultrastructure plays a vital role [2] Similarly, production of novel composites from nanocelluloses [3] and understanding plant growth and function [4] are areas that will benefit greatly from advances in the understanding of the structure of cellulose in the cell wall microfibrils. This situation of insufficient knowledge of the structure is not due to lack of efforts of researchers but rather a consequence of limitations of the analytical methodologies to investigate cell wall structure in situ.[5] Most analytical methods, which provided unique information on cellulose structure, require that prior to analysis cellulose be separated, isolated, and purified. The latter steps, which usually involve thermochemical treatments, can result in the modification of the cellulose native structure by disrupting the delicate originally existent hydrogen bonds. One of the recent comprehensive studies [6] of nanostructure of cellulose in spruce wood microfibrils that used a variety of methods in the experiments favored a 24 chain model of the microfibril and the researchers commented on the locations of the existence of the disordered regions. However, for the purposes of analysis, the microfibrils were assumed to be partly crystalline – a traditional approach. As is clear from the past work and the recently published review,[5] by non-crystalline cellulose the researchers mean that water has access to the molecules of cellulose in the fibril. The criterion is retained in the present investigation.

In this study, based on authors' recent findings [1] where it was demonstrated that cellulose in the native state in wood cell walls was not crystalline, a new model of cell wall cellulose is presented. Additionally, a few implications of the proposed model are explored.

RESULTS AND DISCUSSION

The proposed model is shown in Fig. 1. In this model, along an individual cellulose chain, there are two types of sections – water accessible (curved line section with H-O-H next to it, Fig. 1) and water inaccessible (straight vertical line segment with no H-O-H present next to it, Fig. I). Moreover, the Figure displays some areas that contain symbol "?" next to H-O-H. This symbol designates the uncertainty about water's presence. On the right hand side in Fig. 1, two such microfibrils are represented. The authors are cognizant of the fact that at this stage the model remains simple and as more information is generated, the model may need to be updated.

Interpretation of X-ray Data

Typical WAXS diffractograms of various samples (Table 1, on 4th page; SA7-RT, SA7-OD, SA6, SA17, SA18, SA19) are shown in Fig. 2. Compared to the narrow peaks in the diffractogram of tunicate (e.g., for [200] peak FWHM (full width at half maximum) = 1.0 degrees, Table 1 and Fig. 2), significantly broader peaks were obtained in the case of wood and wood-derived samples ([200] FWHM varies from 2.0 to 3.6 degrees, Table 1 and Fig. 2). Moreover, compared to tunicate cellulose, for the control and variously treated wood samples the [200] peak position was at lower 20 (Table 1 and Fig. 2). Traditionally, both these observations have been explained in terms of contributions of fibril size, hemicellulose, lignin, or amorphous cellulose. However, in light of our model in Fig. 1, there is another possibility and that is of cellulose molecules being present, on average, in aligned but in non-crystalline state which are responsible for these observations ([200] peak position and FWHM). Upon removal of the lateral disorder and consolidation of the cellulose chains the diffractogram would become

sharper and hence, become more comparable to that of tunicate cellulose – which is highly crystalline.

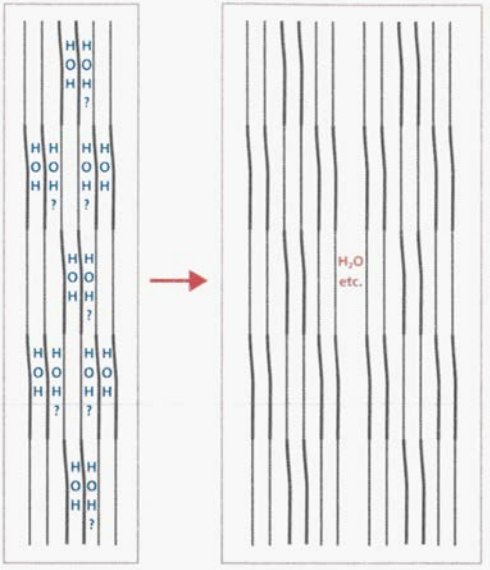

Figure 1. New tentative model of cell wall cellulose based on the authors' work reported elsewhere [1]

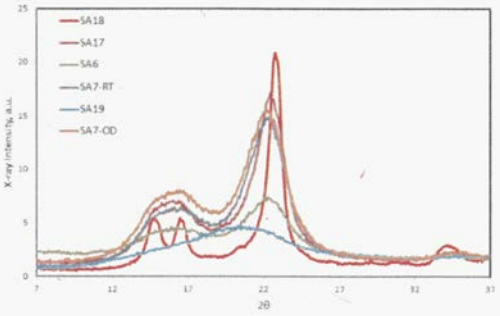

Figure 2. WAXS diffractograms of some cellulose, wood, and treated wood samples.

The previous comments imply that there ought to be a relationship between increased DOLO (lower FWHM) and crystallinity. The plot in Fig. 3 bears this out where Segal-crystallinity was found to be linearly correlated with FWHM (Fig. 3, $R^2 = 0.89$).

Further considering that both, the 1380 cm^{-1} band intensity increase in Raman (D_2O caused, Table 2) and FWHM (XRD, Table 1), were representative of DOLO, the two ought to be related. When such data was plotted for eight common samples in Tables 1 and 2 there was a good correlation between the Raman intensity increase and the FWHM (Fig. 4, $R^2 = 0.95$). This correlation further supported the view that indeed the FWHM represented the degree of order (or disorder) between cellulose chains and suggested that FWHM may have less to do with other factors that are traditionally believed to be the cause (i.e., fibril size, hemicellulose, lignin, or amorphous cellulose). This is an interesting finding and needs further investigation.

Therefore, the proposed model not only explains the accessibility of D_2O to cellulose ([1] and Table 2) but also explains the broadened nature of the X-ray diffractograms.

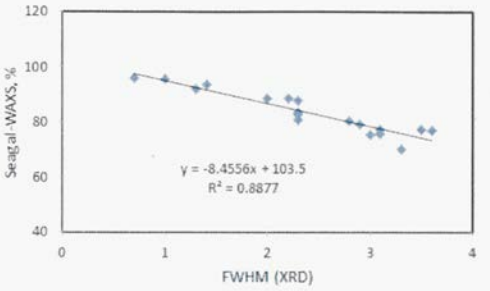

Figure 3. Correlation between FWHM (XRD) and crystallinity (Segal-WAXS).

Table 2. Change in the intensity of Raman band at 1380 cm^{-1} upon OH-to-OD exchange

Sample ID	Sample description	1380 cm^{-1} change[a]
SA2-ND[b]	NaOH treated aspen wood holocellulose,	↑ 75.6 ± 6.5%
SA4-ND	SA4, HCl treated SA2; HCl, 6h @100C;	↑ 36.4 ± 0.8%
SA7-ND	NaOH treated red pine holocellulose	↑ 70.1 ± 2.9%
SA13	Delignified SPORL[c] treated Douglas Fir, #7	↑ 46.2 %
SA17	BNSWKP	↑39.3 ± 2%
SA18	Tunicate cellulose	↓ 1.51 ± 9.6%
SA19	Amorphous cellulose	↑154.3 ± 1.5%
SA20	Pulp-CNCs	↑38.9 ± 4.0%
SA21	Avicel	↑37.7 ± 1.4%
SA22	WhatmanCC31	↑19.0 ± 1%
SA24	Cladophora cellulose	↓ 1.01 ± 1.2%
SA26	Cellulose II; CC31	145 ± 4.0%
SA27	Avicel + 10% xylan	↑37.8 ± 4.0%
SA28	Pulp-CNFs	↑33.6 ± 4.4%

[a]Increase (↑), decrease (↓) compared to intensity in H_2O

[b]Never dried

[c]Sulfite pretreatment to overcome recalcitrance of lignocellulose

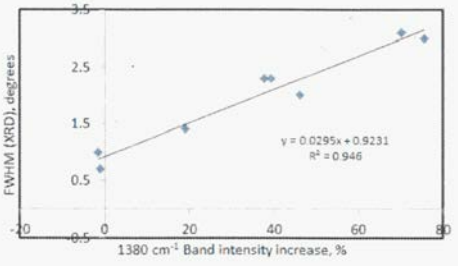

Figure 4. Correlation between D_2O exchange caused Raman intensity increase at 1380 cm^{-1} (Table 2) and FWHM of [200] peak in X-ray diffraction (Table 1).

Other explanations

Although there are numerous other observations in the field of cellulose science that can be explained in terms of the new model, considering the brief nature of this extended abstract, only one more topic will be considered in the following. This has to do with providing an explanation for the results that have showed that not only cellulose crystallinity does not change upon alkaline pulping but also, when kraft-pulps are acid hydrolyzed to cellulose nanocrystals (CNCs;[7]). A limited set of Segal and 380-Raman crystallinity data that was obtained in the laboratory of the authors is listed in Table 3. The Table contains estimated crystallinity data from Segal-WAXS and 380-Raman methods. For woods and pulps, the Segal crystallinities are in the ranges of 76 – 79% and 80 – 85%, respectively. The small differences between the two sets of data can be simply accounted for by a number of possible variations, such as differences between lignin, hemicelluloses, and some consolidation (but no crystallization) of cellulose chains. Similarly, in 380-Raman, the corresponding crystallinities ranges were, 50 – 60% and 50 – 55%, respectively. The 380-Raman method is superior as far as avoiding the influences of lignin and hemicelluloses are concerned. But once again, even in Raman, there is no change in the crystallinity upon pulping (Table 3). Moreover, when pulps are acid hydrolyzed to generate CNCs (Table 3, JY CNCs BEP), once again, no significant change was observed. This observation supported our model which suggests existence of consolidated but non-crystalline regions in pulps, because even when the pulp cellulose is acid hydrolyzed there won't be any increase in cellulose crystallinity. In kraft pulps, the nature of most cellulose chains is similar and compared to wood cellulose, they exist in a state that is more consolidated and H-bonded but not crystalline. Lastly, let's consider the case of heated poplar that seems to have produced slightly higher cellulose crystallinity (in comparison to wood) in the CNCs (Table 3). However, Segal WAXS difference can be explained by the influences of lignin and hemicelluloses and approximately 9 point difference in Raman is probably associated with the consolidation of cellulose chains where reorientation of chains can bring about such an increase. Further work is underway on this topic in the authors' laboratory.

Table 3: Comparison of XRD) and Raman crystallinities, %

Sample ID	Sample description	Segal WAXS		380-Raman	
		Control	CNC	Control	CNC
SA1	Aspen wood, control	77.0	NA	49.9	NA
SA6	Red pine, control	76.8	NA	57.4	NA
SA8	Douglas fir, control	77.0	NA	50.4	NA
SA11	Delig. Douglas Fir, control	79.2	NA	60.9	NA
SA17	BNSWKP	82.5	ND	53.2	ND
SA21	Avicel cellulose	87.5	ND	59.1	ND
AGA-3	Dissolving pulp	87.6	88.2	39.2	46.1
	JY CNCs, BEP[a]	81.8[b] – 84.7	86 - 92	54.8	50 – 57
SA18	Tunicate cellulose	95.6	ND	86.5	73.3
SA19	Amorphous cellulose	23.18	NA	-4.4[f]	NA
SA22	WhatmanCC31	93.5	95.3	82.2	81.8
SA23	Bacterial (FD)	**92.0**	**96.9**	**65.6**	**80.5**
SA24	Cladophora cellulose	95.7	91.6	82.5	74.7
	Poplar, control	69.3	NA	ND	NA
	Heated poplar (170° C)	75.5	91.3	53.2	62

[a]BEP is bleached eucalyptus pulp and the data is taken from [7].

[b]Data was not corrected for any hemicellulose that may have been present.

CONCLUSIONS

A new model based on authors' earlier finding of cell wall cellulose being non-crystalline has been proposed. Using the model, XRDs of some cellulose I materials were explained and an association was made between XRD FWHM and D_2O-induced 1380 cm^{-1} band intensity increase. The model was further relied upon in explaining why the crystallinity of wood cellulose does not increase significantly upon pulping and also upon production of CNCs from pulp.

REFERENCES

[1] Agarwal, U. P.; Ralph, S. A.; Reiner, R. S.; Baez, C. (Submitted for publication).

[2] Sun, Q., et al. *Cellulose*, 2014, **21,** 2419−2431.

[3] Moon, R. J.; Martini, A.; Nairn, J.; Simonsen, J.; Youngblood, *J. Chem Soc Rev* 2011, **40,** 3941−3994.

[4] Cosgrove, D. J. *Nat Rev Mol Cell Biol,* 2005, **6,** 850−861.

[5] Martínez-Sanz, M.; Gidley, J. G.; Gilbert, E. P. *Carbo. Poly.*, 2015, **125,** 120-134.

[6] Fernandes, A. N. et al. *Proc Natl Acad Sci USA,* 2011, **108,** E1195-E1203.

[7] Chen, L.; Wang, Q.; Hirth, K.; Baez, C.; Agarwal, U.P.; Zhu, J.Y. *Cellulose*, 2015, **22,** 1753–1762.

Table 1. Crystallinity (Segal-WAXS and Raman), XRD [200] peak position and FWHM of various samples

Sample ID	Sample description	Crystallinity[a], %		[200] peak position	[200] FWHM
		Segal-WAXS	Raman[b]		
SA1	Aspen wood, control	77.0	49.9	22.5	3.1
SA2-RT	NaOH treated aspen holocellulose, RT	75.3	47.9	22.2	3.0
SA2-OD	NaOH treated aspen holocellulose, OD	80.1	ND[c]	22.3	2.8
SA6	Red pine, control	76.8	57.4	22.5	3.6
SA7-RT	NaOH treated red pine holocellulose, RT	75.5	56.6	22.2	3.1
SA7-OD	NaOH treated red pine holocellulose, OD	70.1	ND	22.2	3.3
SA8	Douglas fir, control	77.0	50.4	22.5	3.5
SA9	SPORL treated Douglas fir, #3	83.4	ND	22.7	2.3
SA10	SPORL treated Douglas fir, #7	80.7	ND	22.7	2.3
SA11	Delig. Douglas Fir, control	79.2	60.9	22.6	2.9
SA12	Delig. SPORL treated Douglas Fir, #3	88.3	ND	22.7	2.2
SA13	Delig. SPORL treated Douglas Fir, #7	88.3	52.6	22.7	2.0
SA17	BNSWKP[d]	82.5	53.2	22.4	2.3
SA18	Tunicate cellulose	95.6	86.5	22.8	1.0
SA19	Amorphous cellulose	23.18	-4.4	20.7	NA[e]
SA21	Avicel cellulose	87.5	59.1	22.7	2.3
SA22	WhatmanCC31	93.5	82.2	22.7	1.4
SA23	Bacterial cellulose	92.0	65.6	22.7	1.3
SA24	Cladophora cellulose	95.7	82.5	22.9	0.7

[a]In the context of the present investigation, for wood and wood-derived samples, FWHM (XRD) can be considered as "degree of lateral order'' or DOLO.
[b]Where needed, Raman values are corrected for hemicellulose contribution.
[c]Not done
[d]Bleached northern softwood kraft pulp
[e]Not applicable